Structural, Optical and Laser Damage Threshold Studies of Polarizable Organic Crystal: 4-Methylpyridinium Picrate

D. Shalini, V. Revathi Ambika, N. Hema, R. Usha and D. Jayalakshmi[*]

PG and Research Department of Physics, Queen Mary's College (A), Chennai-600 004, India

*Corresponding author: E-mail: djayalakshmi2016@gmail.com

New organic material has been synthesized and single crystals were grown from aqueous solution. Single crystals of 4-methylpyridinium picrate have been grown by slow evaporation technique acetone as a solvent at room temperature. Single crystal X-ray diffraction study on grown crystals shows that it belongs to monoclinic system. Fourier transform infrared (FTIR) spectroscopic study was performed for the identification of different modes of functional groups present in the compound. The thermal stability of the compound has been determined by TG-DTA curves. The result shows that the material starts decomposing at 171.50 °C. The UV-visible transmission spectrum has been recorded in the range 190-900 nm. The photoconductivity study confirms the negative photoconductive nature of the sample. The dielectric measurement of the compound has been analyzed using dielectric analysis. Laser damage threshold value for the crystal was measured.

Keywords: 4-Methylpyridinium picrate, Monoclinic, Transmission, Laser damage threshold.

INTRODUCTION

The crystalline material is very essential for the expansion of non-linear optical field and the continuous detection of different effective and well-organized nonlinear equipments. It encourages the wide applications of laser frequency conversion techniques in many areas [1]. Organic molecules containing donor and acceptor groups have new advantages over inorganic materials due to the possibility of enhanced electronic non-linear optical polarization response [2]. Hydrogen bonding defines the structure of the crystals so this plays an important role in molecular recognition and crystal engineering research [3]. Pyridine derivatives are present in large molecules that it allows us to obtain different substituents in any positions on the pyridine ring and several pyridine derivatives possess optical properties [4,5]. Picric acid forms crystalline picrates of different organic molecules through ionic and hydrogen bonding. In this work 4-methypyridinium picrate (4MPI) is one such donor acceptor molecular compound in which 4-methypyridinium acts as acceptor and the picric acid act as a donor.In the present investigation, we report synthesis, growth, structural, spectral, optical, dielectric and thermal properties of 4-methylpyridinium picrate single crystal.

EXPERIMENTAL

Growth process: The grown crystals were obtained by the method of slow evaporation technique at room temperature.

The 4-methylpyridine and picric acid taken in a 1:1 molar ratio. Picric acid is dissolved in 100 mL of acetone using magnetic stirrer, following which 4-methyl pyridine (Sigma Aldrich) solution is being added with drop by drop. The stirring is allowed up to 6 h to attain the saturation state of the solution. The prepared solution is filtered using Whatman filter paper and then the solution is kept at room temperature, without any disturbance from the environment. 4-Methylpyridinium picrate crystal has been obtained within 2-3 weeks and the grown crystal is allowed to recrystallization process to improve the optical quality of the crystal. The grown 4-methyl-pyridinium picrate crystal is shown in Fig. 1.

Fig. 1. As-grown crystal of 4-methylpyridinium picrate

FT-IR: The FT-IR spectrum is recorded between 4000-400 cm^{-1} using KBr pellet technique by Bruker IFS 66V FT-IR spectrometer.

Measurement of melting point: The melting point of 4-methylpyridinium picrate compound is 159 °C. The error of the measurement was ± 2 °C.

Thermal analysis: Thermo gravimetric analysis (TGA) and differential thermal analysis (DTA) of grown crystals (4-methylpyridinium picrate) were carried out simultaneously by employing TA instrument model Q600 SDT thermal analyzer. The sample was heated at the rate of 10 °C/min in inert nitrogen atmosphere.

UV-Vis-NIR analysis: The optical studies for 4-methyl-pyridinium picrate crystals were carried out using T-90+ Lab India UV-visible spectrophotometer in the range 190-900 nm.

X-ray diffraction analysis: The crystal of 4-methyl-pyridinium picrate was confirmed by single crystal X-ray diffraction analysis using Bruker kappa APEXII single crystal X-ray diffractometer with graphite monochromated MoKα radiation (λ = 0.71073 Å) at 296 K.

Refractive index measurement: Polished crystals of the 4-methylpyridinium picrate were used for refractive index measurements. These crystals were placed on a rotating mount at an angle from 0 to 90°. He-Ne laser of wavelength 632.8 nm was used as the source. Brewster's angle (θp) for 4-methyl-pyridinium picrate was measured to be 56.6°. The refractive index has been calculated using the equation n = tan θp, where θp is the polarizing angle and it is found to be 1.52.

Photoconductivity studies: The photoconductivity studies of the grown crystals were carried out by connecting the sample in series with a DC power supply and a pico ammeter (Kiethley 485) at room temperature. The crystal was covered with a black cloth and the applied voltage was increased from 0 to 300 Volts in steps of 20 Volt and the dark current was recorded. The sample was illuminated by the radiation from 100 W halogen lamp containing iodine vapour and tungsten filament. The photocurrent was recorded for the same values of the applied voltage.

Dielectric analysis: Good quality single crystals of 4-methylpyridinium picrate crystal were selected for the dielectric measurements using HIOKI3532-50 LCR HITESTER in the frequency range of 50 Hz to 5 MHz at various temperatures like 40, 50, 60 and 70 °C.

Laser damage threshold studies: The LDT measurement was made on the finely polished 4-methylpyridinium picrate crystal having thickness of 1 mm. Experimentally, a Q-switched diode array side pumped Nd:YAG laser operating at 532 nm radiation was used for this study. Many shot LDT measurements were made on the well polished plane of the grown 4-methylpyridinium picrate crystal. The beam spot size on the sample was 1 mm and input energy was measured as 350 mJ. The energy density of the input laser beam was recorded using power meter till the crystal got damaged.

RESULTS AND DISCUSSION

X-ray diffraction analysis: Single crystal XRD analysis of 4-methylpyridinium picrate reveals that the crystal crystallizes in monoclinic crystal system with space group P2₁. The asymmetric unit of the 4-methylpyridinium picrate consists of the four picrate anions and four pyridinium cations. The protonation on the N_4 site of the cation is confirmed from C-N bond distances and C-N-C bond angles. All the bond distances and bond angles of the four molecules in the asymmetric unit agreed with each other. In the crystal the cations are linked to anions *via* bifurcated N–H⋯ (O,O) hydrogen bonding which generating R_1^2 (6) graph motif. The N–H⋯O bonding is highly responsible for stability of the molecule. The torsion angles C37-C38-C39-C40 = 179.2(5)° and C42-C41-C39-C40 = -179.5(5)°, which shows that the methyl group is in the +anti-periplanar (+ap) orientation with pyridinium ring. The dihedral angle between the pyridinium cations and picrate anions ring is 2.97°, which shows axial orientation between each other's [6-8].

Table-1 shows the data and refinement of the X-ray crystal structure determination for this compound. Selected bond lengths and bond angles are presented in Table-2. ORTEP (Fig. 5) and the interaction of a single salt molecule view with numbering scheme in Fig. 4 and packing diagram (1 and 2) is shown in Figs. 2 and 3. The observed hydrogen bonds of 4-methyl-pyridinium picrate compound are summarized in Table-3.

TABLE-1
CRYSTALLOGRAPHIC AND STRUCTURE REFINEMENTS DATA OF 4-METHYLPYRIDINIUM PICRATE

Empirical formula	$C_{28}H_{24}N_{10}O_6$
Formula weight	596.57
Temperature	293(2) K
Wavelength	0.71073 Å
Crystal system, space group	Monoclinic, P2₁
Unit cell dimensions	a = 7.3088(1) Å, α = 90°
	b = 24.886(1) Å, β = 90.567°
	c = 15.039 (1) Å, γ = 90°
Volume	2735.3 (2) A³
Z, Calculated density	4, 1.449 Mg/m³
Absorption coefficient	0.106 mm⁻¹
F(000)	1240
Crystal size	0.30 × 0.20 × 0.20 mm
Theta range for data collection	1.35 to 26.02 °
Limiting indices	-8 <= h <= 8;
	-30 <= k <= 30;
	-18 <= l <= 18
Reflections collected/unique	39220/10699 [R(int) = 0.0556]
Completeness to θ = 26.02	99.7 %
Refinement method	Full-matrix least-squares on F²
Data/restraints/parameters	10699/1/824
Goodness-of-fit on F²	1.045
Final R indices [I > 2σ(I)]	R1 = 0.0653, wR2 = 0.1527
R indices (all data)	R1 = 0.1282, wR2 = 0.1935
Absolute structure parameter	1.5 (2)
Largest diff. peak and hole	0.424 and -0.342 e.A⁻³

FT-IR analysis: In 4-methylpyridinium picrate, there was a formation of strong hydrogen bond between 4-methylpyridine and picric acid. The anion donates from picric acid to pyridine moiety to form N⁺-H bond. The peak observed at 3434 cm^{-1} is due to N-H stretching vibrations (Fig. 6). The phenolic C-O stretching vibrations of picric acid is observed at 1297 cm^{-1}. The peak observed at 3072 cm^{-1} corresponds to the aromatic C-H stretching. The C-C stretching vibrations at 1589 cm^{-1} has been identified and assigned. The characteristic peak at

TABLE-2 SELECTED BOND DISTANCES (Å) AND BOND ANGLES (°) OF 4-METHYLPYRIDINIUM PICRATE			
Bond distances		Bond angles	
C(7)-C(8)	1.382(1)	C(8)-C(7)-C(12)	124.4(1)
C(7)-N(5)	1.447(1)	N(5)-C(7)-C(12)	119.7(1)
C(7)-C(12)	1.452(1)	C(9)-C(8)-C(7)	117.6(1)
C(8)-C(9)	1.367(1)	C(8)-C(9)-C(10)	122.6(1)
C(9)-C(10)	1.378(1)	C(8)-C(9)-N(7)	116.6(1)
C(9)-N(7)	1.432(1)	C(10)-C(11)-C(12)	125.0(1)
C(10)-C(11)	1.352(1)	C(10)-C(11)-N(6)	115.8(1)
C(11)-C(12)	1.431(1)	N(4)-C(42)-C(41)	119.0(1)
C(11)-N(6)	1.462(1)	C(37)-C(38)-C(39)	120.5(1)
C(12)-O(1)	1.244(1)	O(1)-C(12)-C(11)	123.6(1)
C(37)-N(4)	1.339(1)	O(3)-N(5)-O(2)	121.6(1)
C(37)-C(38)	1.364(1)	O(3)-N(5)-C(7)	117.9(1)
C(38)-C(39)	1.376(1)	N(4)-C(37)-C(38)	119.6(1)
C(39)-C(41)	1.382(1)	O(7)-N(6)-O(6)	122.9(1)
C(39)-C(40)	1.491(1)	O(4)-N(7)-O(5)	121.6(1)
C(41)-C(42)	1.362(1)	–	–
C(42)-N(4)	1.323(1)	–	–
N(4)-H(4)	0.8600	–	–

Fig. 2. Packing 1 for 4-methylpyridinium picrate

Fig. 3. Packing 2 for 4-methylpyridinium picrate

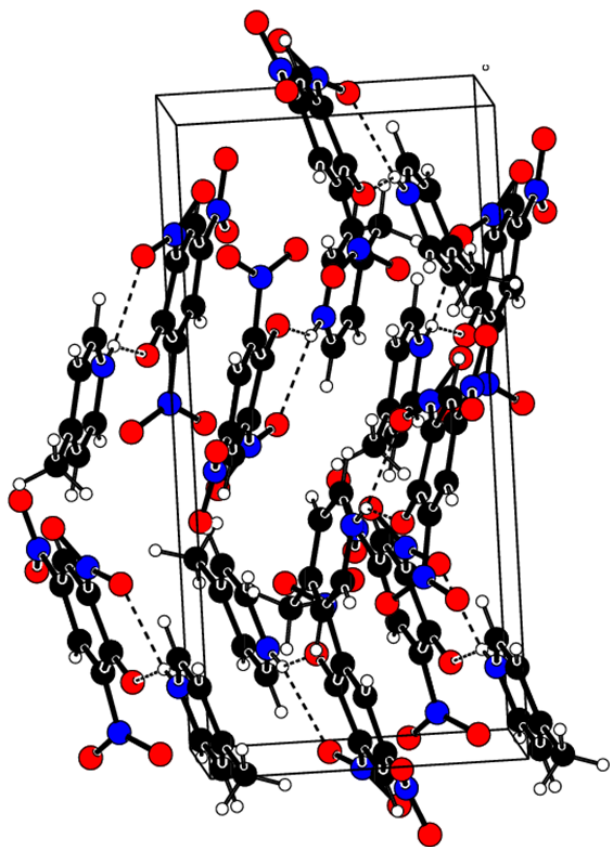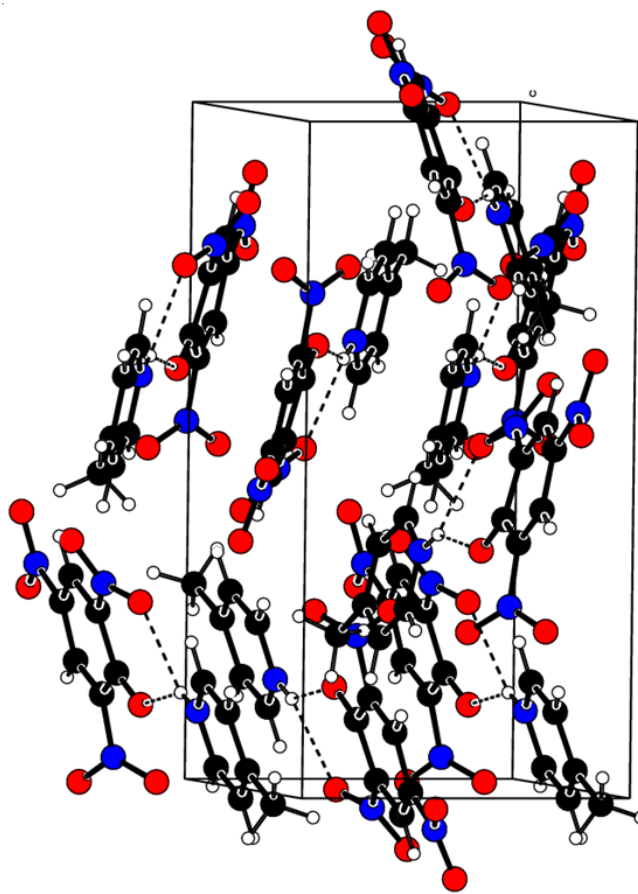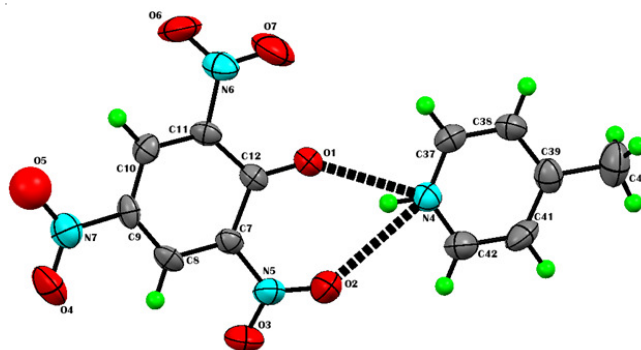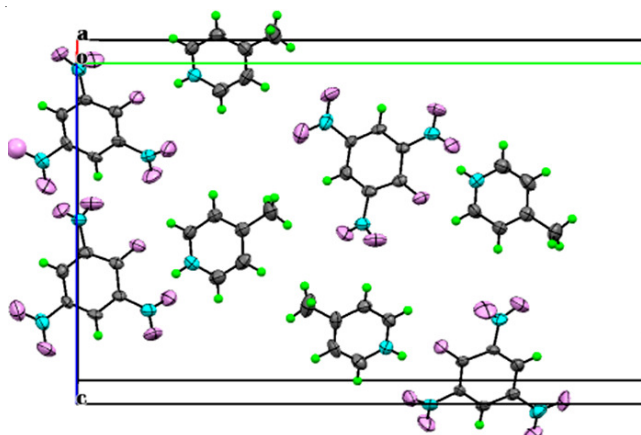Fig. 4. Labeled diagram of 4-methylpyridinium picrate. Thermal ellipsoidal 50 % probability level
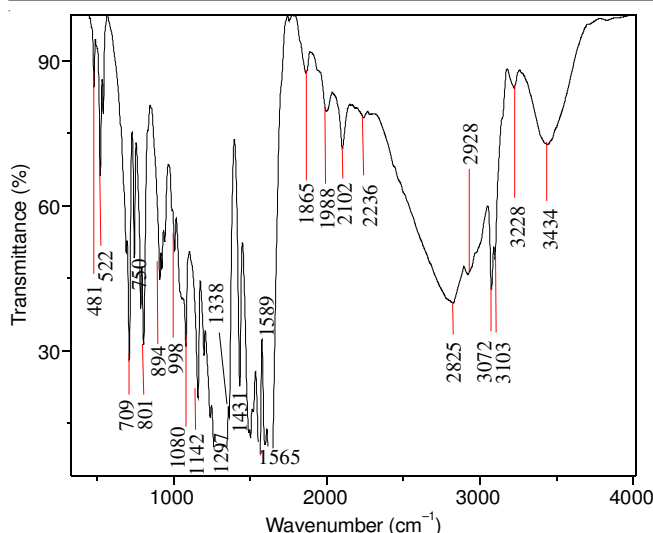

Fig. 5. ORTEP plot for 4-methylpyridinium picrate

1431 cm^{-1} is due to the ring stretching vibration of C=C group. The asymmetric and symmetric stretching vibration of NO$_2$ is observed at 1565 and 1338 cm^{-1}. The ring stretching of C=N group is observed at 1431 cm^{-1}. The peak at 998 cm^{-1} due to the in-plane C-H bending. The out-of-plane C-H bending of aromatic compound is observed at 750 cm^{-1}. The ring C=C bending is observed at 709 cm^{-1}. The peak at 522 cm^{-1} is due to NO$_2$ rocking [9]. Table-4 shows FT-IR Spectral data of 4-methylpyridinium picrate crystal.

Fig. 6. FTIR spectrum of 4-methylpyridinium picrate

Fig. 7. TG-DTA curves for 4-methylpyridinium picrate

TABLE-3
HYDROGEN BONDS GEOMETRY OF 4-METHYLPYRIDINIUM PICRATE

D-H···A	d(D-H) (Å)	d(H···A) (Å)	d(D···A) (Å)	∠(DHA) (°)
N(4)-H(4)···O(1)#1	0.86	1.93	2.673(1)	143.5
N(4)-H(4)···O(2)#1	0.86	2.22	2.883(1)	134.3
Symmetry codes: x-1/2,-y, z+1/2 #1				

TABLE-4
FT-IR SPECTRAL DATA OF 4-METHYLPYRIDINIUM PICRATE

Frequencies (cm⁻¹)	Assignment
3434	N⁺-H stretching
3072	C-H stretching
1297	Phenolic C-O stretching vibrations of picric acid
1589	C-C stretching vibration
1431	C=C stretching vibration
1565 & 1338	Asymmetric and symmetric stretching vibrations of NO₂
998	In-plane C-H bending
750	Out-of-plane C-H bending of aromatic compound
522	NO₂ rocking

Thermal analysis: From TGA curve (Fig. 7) of 4-methyl-pyridinium picrate was observed to be at 171.50 °C with no weight loss. It is clear that there is no physically absorbed water content in the molecular structure of 4-methylpyridinium picrate compound. Since TGA curve shows a single stage weight loss due to decomposition of 4-methylpyridinium picrate into fragments and its subsequent volatilization. An endothermic peak is observed in DTA at 170.05 °C which is due to melting of the sample. Further it indicates that there is no phase transition before this melting point and also the grown crystal is free from solvent inclusion. Good crystalline nature of the 4-methylpyridinium picrate compound is clearly evident from the sharpness of the endothermic peak [10].

UV-Vis-NIR analysis: Fig. 8 shows the transmittance spectra of the grown crystal. When transmission is monitored from longer wavelength to shorter wavelength, hence there is no absorption between the regions from 900 to 435 nm. The lower cut-off wavelength is found to be 435 nm and the
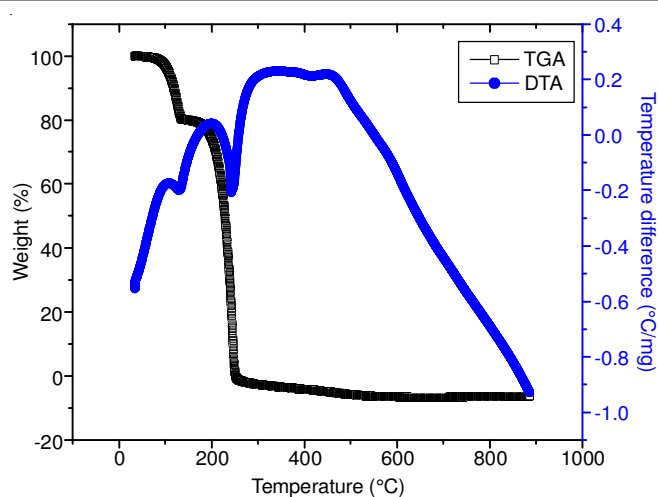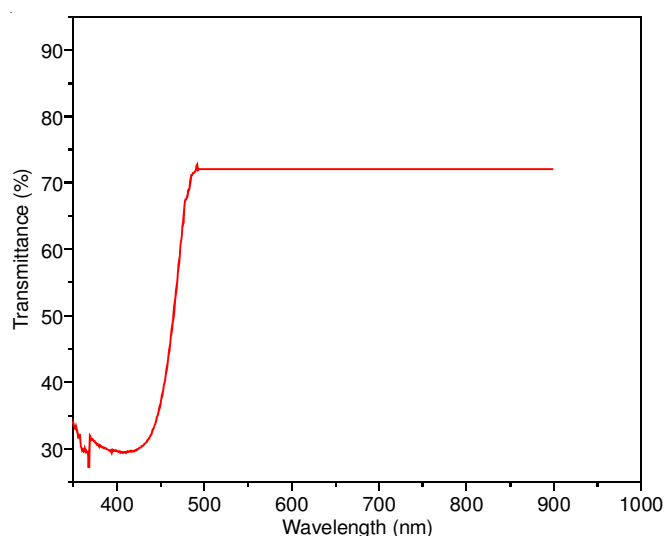

Fig. 8. UV-visible spectrum of 4-methylpyridinium picrate

percentage of transmittance is 72 %. An electron under impact by an incident photon is excited to middle state where it interacts with lattice vibrations and it reaches a final state, the entire result being the absorption of photons [11]. The absorption coefficient (α) was calculated from the transmission spectrum based on the following equation:

$$\alpha = \frac{1}{t}\log\left(\frac{1}{T}\right) \tag{1}$$

where, T is the transmittance and 't' is the thickness of crystal.

It also ensures the crystal suitability for optical harmonic generation, optoelectronic device application [12].

Photoconductivity studies: Fig. 9 shows dark and photo currents dependence of field. It revealed that the dark current and photo current increase linearly with applied field. Hence, 4-methylpyridinium picrate crystal has more dark current than the photo current, called as negative photoconductivity. The negative photoconductivity in this case is due to the reduction of the number of charge carriers or their life time in the presence of radiation [13]. Life time decreases with illumination, could be due to the trapping process and increase in carrier velocity according to the relation,

$$\tau = (vsN)^{-1} \qquad (2)$$

where, v is the thermal velocity of the carriers, s is the capture cross section of the recombination centers and N is the carrier concentration [14]. As a result, the sample is kept under exposure to light, the recombination of electrons and holes take place, resulting in decrease in the number of mobile charge carriers, giving rise to negative photoconductivity.
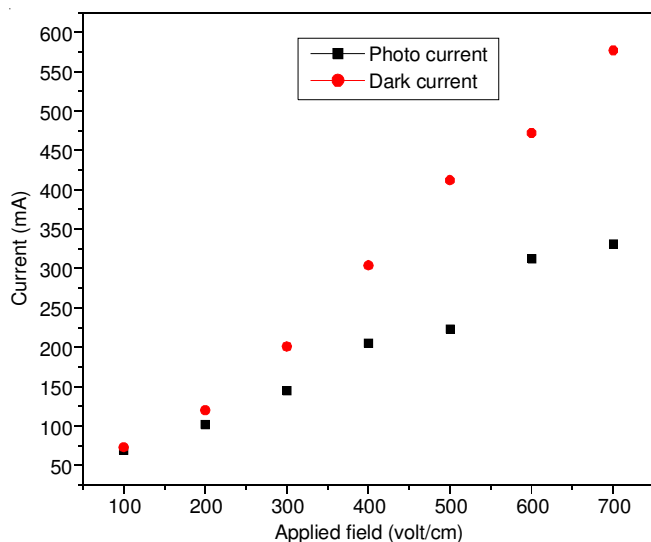

Fig 9. Variation of current with applied field for 4-methylpyridinium picrate crystal

Dielectric analysis: Figs. 10 and 11 shows the dielectric constant and dielectric loss for different frequencies. These curves proposed that the dielectric loss strongly depends on the frequency of applied field, similar to that of dielectric constant which is common for the ionic system of crystals [15,16]. In organic compound, the dielectric response is excellent in the lower frequency region and hence the experiments were carried out in the lower frequency region only. The dielectric constant (ε_r) was calculated using the following equations:

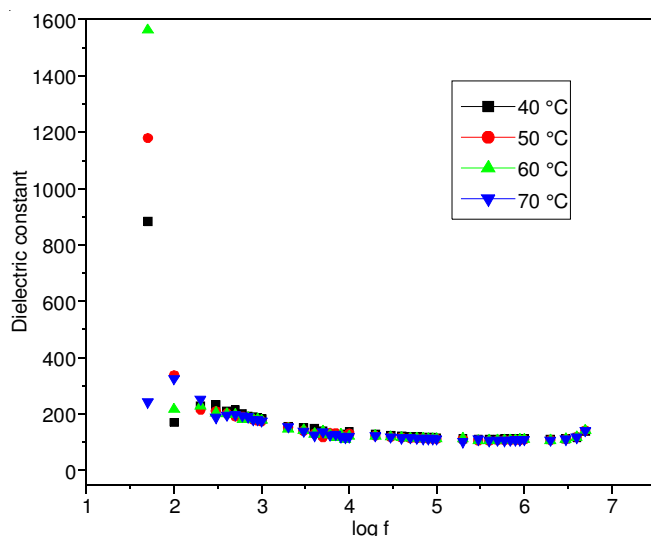$$\varepsilon_r = \frac{C_{crys}}{C_{air}} \qquad (3)$$

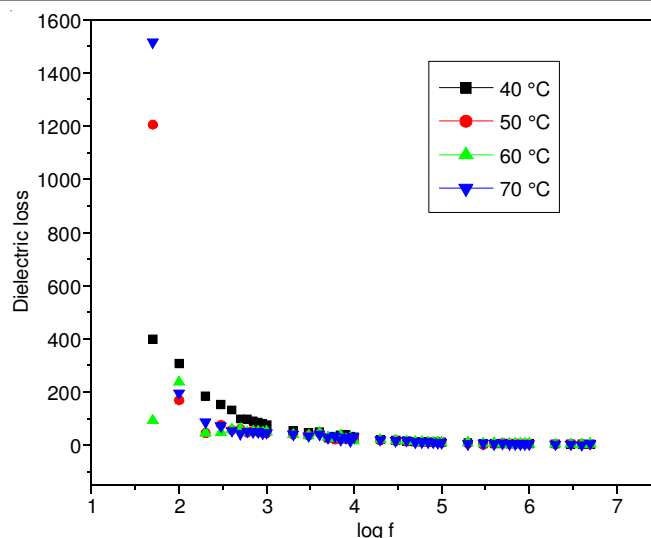Fig. 10. Dielectric constant *vs.* frequency

Fig. 11. Dielectric loss *vs.* frequency

$$\varepsilon_r = \frac{Ct}{\varepsilon_0 A} \qquad (4)$$

where, C is the capacitance; t is the thickness of the sample; ε_0 is the permittivity of the free space and A is the area of cross section.

The dielectric loss was calculated using the following relation:

$$\varepsilon'' = \varepsilon_r D \qquad (5)$$

where, D is the dissipation factor.

From the graph the dielectric constant decreases at high frequencies is recognized to the significant decrease in all the three polarizations such as orientation, electronic and ionic polarization and presence of space charge polarization near the grain boundry interface [17]. In 4-methylpyridinium picrate compound the value of dielectric constant at lower frequencies due to the excitation of the lattice vibrations and space charge polarization. The low value of dielectric constant at higher frequencies could be predictable to the declining of these polarizations slowly and contributed mainly by electronic polarization. The low dielectric loss at high frequency indicate that the grown 4-methylpyridinium picrate contains minimum defects [18,19].

Laser damage threshold studies: The laser damage threshold depends upon the optical absorption, properties of materials, pulse width and specific heat, *etc*. If the laser damage threshold will be high, the material has high specific heat. If the material has a low laser damage threshold it strictly restricts its applications, like high optical transmittance [20]. The laser damage mainly occurs due to strain induced fractures caused by ionization processes and multi-photon absorption. The surface damage threshold of the crystal was calculated using the formula:

$$\text{Power density (d)} = E/\tau A \qquad (6)$$

where, E is the energy (mJ), τ is the pulse width (ns) and A is the area of the circular spot size. The calculated laser damage threshold is 6.96 GW/cm². The LDT value of 4-methyl-pyridinium picrate crystal was high when compared to already report materials and the comparison value is shown in Table-5. Hence,

TABLE-5
COMPARISON OF LASER DAMAGE THRESHOLD
VALUE WITH WELL-KNOWN CRYSTALS

Crystal name	LDT value (GW/cm^2)	Ref.
Benzimidazole by SEST	1.71	[21]
Benzimidazole by VBT	2.86	[21]
2-Aminopyridinium succinate succinic acid	0.80	[22]
3-Br-4'-Methoxychalcone	0.90	[23]
4-Methylpyridinium 4-hydroxybenzoate	5.41	[24]
4-Methylpyridinium picrate	6.96	Present work

SEST = Slow evaporation solution growth technique.
VBT = vertical Bridgman technique.

it is clear that the grown 4-methylpyridinium picrate crystal with high LDT value can be used for high-power laser device fabrications.

Conclusion

Crystals of 4-methylpyridinium picrate were grown by slow evaporation solution growth technique and the monoclinic crystal system was confirmed in the single XRD studies. Functional groups were identified by analyzing infrared spectrum and the impacts of hydrogen bonds on the vibration of functional groups were studied. Thermal analysis confirms that the crystal is stable upto 170.50 °C. Optical studies shows the transparency nature of the crystal and it enhances the suitability of the material for opto-electronic applications. The photocurrent was less than the dark current signifying negative photoconducting nature. The low dielectric constant at higher frequency region indicates that the grown material is appropriate for electro optic applications. High value of laser damage threshold was measured.

REFERENCES

1. X.-T. Wu and L. Chen, Structure-Property Relationships in Non-Linear Optical Crystals II, Springer, vol. 145 (2012).
2. P.V. Dhanaraj, N.P. Rajesh, G. Vinitha and G. Bhagavannarayana, *Mater. Res. Bull.*, **46**, 726 (2011); https://doi.org/10.1016/j.materresbull.2011.01.013.
3. N.C. Khalib, K. Thanigaimani, S. Arshad and I.A. Razak, *Acta Crystallogr. Sect. E Struct. Rep. Online*, **69**, o1120 (2013); https://doi.org/10.1107/S1600536813016310.
4. M.A. Rajkumar, N.N. Mohideen, S.S.J. Xavier, S. Anbarasu and D.P.A. Devarajan, *Acta Crystallogr. Sect. E Struct. Rep. Online*, **71**, 231 (2015); https://doi.org/10.1107/S2056989015000365.
5. F. Brody and P.R. Ruby, in ed.: E. Klingsberge, Pyridine and its Derivatives, Interscience, New York, vol. 114, p. 289 (1960).
6. Bruker, APEX2, SAINT, XPREP and SADABS Bruker AXS Inc, Madison, Wisconsin, USA (2004).
7. G.M. Sheldrick, SHELXS97 and SHELXL97, University of Gottingen, Germany (1997).
8. G.M. Sheldrick, *Acta Crystallogr. A*, **64**, 112 (2008); https://doi.org/10.1107/S0108767307043930.
9. R.M. Silverstein, G.C. Bassler and T.C. Morrill, Spectrometric Identification of Organic Compounds, Wiley, New York (1991).
10. A.S.H. Hameed, G. Ravi, R. Dhanasekaran and P. Ramasamy, *J. Cryst. Growth*, **212**, 227 (2000); https://doi.org/10.1016/S0022-0248(99)00896-9.
11. M. Mersch, K. Buse, W. Sauf, H. Hesse and E. Kratzig, *Phys. Status Solidi*, **140**, 273 (1993); https://doi.org/10.1002/pssa.2211400127.
12. D.D.O. Eya, A.J. Ekpunobi and C.E. Okeke, *Acad. Open Internet J.*, **17**, 1 (2006).
13. R.H. Bube, Photoconductivity of Solids, Wiley, New York (1981).
14. I.M. Ashraf, H.A. Elshaikh and A.M. Badr, *Cryst. Res. Technol.*, **39**, 63 (2004); https://doi.org/10.1002/crat.200310150.
15. K.V. Rao and A. Smakula, *J. Appl. Phys.*, **36**, 2031 (1965); https://doi.org/10.1063/1.1714397.
16. K.V. Rao and A. Smakula, *J. Appl. Phys.*, **37**, 319 (1966); https://doi.org/10.1063/1.1707834.
17. G. Prabagaran, S. Arulmozhi, M.D. Raja and J. Madhavan, *IOSR J. Appl. Phys.*, **2**, 51 (2013).
18. K.B.R. Varma, K.B. Ramanaiah and K.V. Rao, *Bull. Mater. Sci.*, **5**, 39 (1983); https://doi.org/10.1007/BF02822348.
19. P. Rajesh and P. Ramasamy, *J. Cryst. Growth*, **311**, 3491 (2009); https://doi.org/10.1016/j.jcrysgro.2009.04.020.
20. J.A. Brant, D.J. Clark, Y.S. Kim, J.I. Jang, A. Weiland and J.A. Aitken, *Inorg. Chem.*, **54**, 2809 (2015); https://doi.org/10.1021/ic502981r.
21. N. Vijayan, G. Bhagavannarayana, R. Ramesh Babu, R. Gopalakrishnan, K.K. Maurya and P. Ramasamy, *Cryst. Growth Des.*, **6**, 1542 (2006); https://doi.org/10.1021/cg060002g.
22. M. Magesh, G. Bhagavannarayana and P. Ramasamy, *Spectrochim. Acta Mol. Biomol. Spectrosc*, **150**, 765 (2015); https://doi.org/10.1016/j.saa.2015.05.077.
23. P.S. Patil, S.M. Dharmaprakash, K. Ramakrishna, H.-K. Fun, R.S.S. Kumar and D.N. Rao, *J. Cryst. Growth*, **303**, 520 (2007); https://doi.org/10.1016/j.jcrysgro.2006.12.068.
24. S. Sudhahar, M.K. Kumar, B.M. Sornamurthy and R.M. Kumar, *Spectrochim. Acta Part A: Mol. Biomol. Spectrosc.*, **118**, 929 (2014); https://doi.org/10.1016/j.saa.2013.09.072.